Acta Cryst. (1971). A27, 408

A Method of Predicting Line Shapes in Three-Axis Spectrometry

BY B. C. HAYWOOD

Materials Physics Division, A.E.R.E., Harwell, Berkshire, England

(*Received* 16 *November* 1970)

A simple formulation is described which can be used to predict the line shape obtained in three-axis spectrometry. The method is shown to produce curves in good agreement with measured data.

The resolution function for a three-axis spectrometer has recently been derived by Cooper & Nathans (1967) in the form of a probability distribution in the four dimensions, $k_x k_y k_z$ and ω, of momentum–energy space. With the spectrometer adjusted to look at the point $\mathbf{Q},\omega$ in this space, the resolution function is

$$R(X_1,X_2,X_3,X_4)=\exp\left[-\left(\sum_{i=1}^{4}\sum_{j=1}^{4}X_iA_{ij}X_j\right)\right] \qquad (1)$$

where X_{1-3} are the x, y and z components of $\Delta\mathbf{Q}$ and X_4 is $\Delta\omega$. The origin of the coordinates of the vector $\mathbf{X}[=(X_1,X_2,X_3,X_4)]$ is thus the point $\mathbf{Q},\omega$. A_{ij} is a 4×4 symmetric matrix.

The number of neutrons scattered into the detector will thus be proportional to

$$I=\int\int\int\int R(X_1,X_2,X_3,X_4)D(X_1,X_2,X_3,X_4)\prod_{i=1}^{4}\mathrm{d}X_i \qquad (2)$$

where $D(\mathbf{X})$ is the cross section at the point $\mathbf{X}$. The result of adjusting the spectrometer so that the point under investigation moves in a series of discrete steps along a path in momentum–energy space can be predicted by evaluating I for the points along this path. Programs have been written to evaluate these integrals for various types of cross section, but except in certain special cases, each integration has to be performed numerically, involving a considerable amount of computation.

One of the interesting types of cross section is that for a perfect elastic solid, in which the cross section is constant for values of $\mathbf{Q}$ and ω lying on a surface in momentum–energy space and zero elsewhere. If the equation of this dispersion surface is $f(\mathbf{Q},\omega)=0$ then the cross section is proportional to the delta function $\delta[f(\mathbf{Q},\omega)]$.

The scattered neutron intensity, equation (2), may then be written

$$I=\int\int\int\int R(\mathbf{X})\delta[f(\mathbf{X})]\prod_{i-1}^{4}\mathrm{d}X_i \qquad (3)$$

The evaluation of this integral may be carried out in several ways. The equation for the dispersion surface could be used to reduce the number of variables in the integration from four to three and the integration could then be carried out numerically. This would still lead to a considerable amount of computation. The approach adopted in this present work is to replace the delta function by its analytic form,

$$\delta[(f\mathbf{X})]=\frac{1}{2\pi}\int_{-\infty}^{\infty}\exp\left(-i\mu f(\mathbf{X})\right)\mathrm{d}\mu \qquad (4)$$

where μ is a dummy variable. If now the dispersion surface can be represented by a quadratic equation in ω and Q the number of integrals which need to be evaluated numerically is reduced to one.

The general four-dimensional quadratic equation may be written

$$\sum_{i=1}^{4}\left(\sum_{j=1}^{4}X_iB_{ij}X_j+T_iX_i\right)+H=0 \qquad (5)$$

where $\mathbf{B}$ is a 4×4 symmetric matrix, $\mathbf{T}$ is a four-component vector and H is a constant. We may now write (2) in terms of equations (5) and (1) as

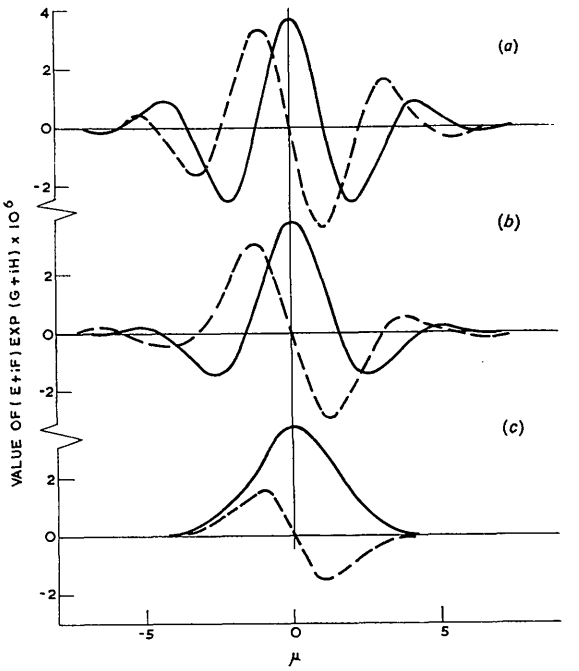

Fig. 1. The integrand of equation (7) for the neutron group shown in Fig. 2 at the energy values (*a*) 0·7, (*b*) 1·0 and (*c*) 1·3 THz. The solid line is the real part and the dashed line the imaginary part.

$$I(\mathbf{X}^0)=\int\int\int\int\int\int \exp -\left\{\sum_{i=1}^{4}\left(\sum_{j=1}^{4}[X_iA_{ij}X_j + i\mu(X_i+X_i^0)B_{ij}(X_j+X_j^0)]\right) + i\mu T_i(X_i+X_i^0)+i\mu H\right\}\prod_{i=1}^{4} \mathrm{d}X_i\mathrm{d}\mu\,. \quad (6)$$

In this equation the origin of the resolution function is at the point $\mathbf{X}^0$ in the coordinates of the dispersion surface.

The integration over $\mathbf{X}$ may now be performed analytically and the result is

$$I(\mathbf{X}^0)=\int_{-\infty}^{\infty}(E+iF)\exp(G+iK)\mathrm{d}\mu \quad (7)$$

where E, F, G and K are functions of $\mathbf{X}^0$ and μ given in the Appendix.

This integral can be shown to converge and at large values of μ, E and F go as μ^{-2} and G tends to a constant. The function to be integrated is symmetric in $+$ and $-\mu$ and consists of a damped oscillatory function whose main area comes from the lobe centred at $\mu=0$. The height of this lobe is independent of the shape of the dispersion surface as can be seen from equation (6) and the effect of passing the resolution probability function through the surface can be seen in Fig. 1 showing the integrand of equation (7) and Fig. 2 showing $I(\mathbf{X}^0)$. In Fig. 1(*a*) the probability function is centred well away from the dispersion surface, and $I(\mathbf{X}^0)$ [equation (7)] has value close to zero. As the resolution function approaches the dispersion surface the centre lobe broadens as in Fig. 1(*b*) where the value of $I(\mathbf{X}^0)$ is still small but finite, until finally the peak of the intensity distribution is reached as in Fig. 1(*c*). The imaginary part of the integral is antisymmetric about $\mu=0$ and thus sums to zero.

The fit of $I(\mathbf{X}^0)$ to typical experimental data can be seen in Fig. 2. The points are those for a longitudinal

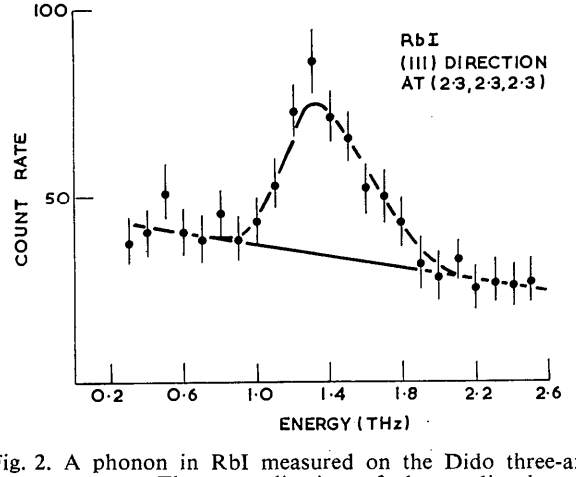

Fig. 2. A phonon in RbI measured on the Dido three-axis spectrometer. The normalization of the predicted curve (dashed line) has been made to the area under the experimental points.

phonon in RbI travelling along the [111] direction Saunderson (private communication).

The most serious limitation to the applicability of this method is that it is not possible to include in the equation terms of the form $1/\omega$ or $1/\omega^2$, which are found in the cross section equations for magnons and phonons. This limitation arises from the original assumption of Cooper & Nathans that the collimator transmission functions and crystal-mosaic spreads may be described by Gaussian distributions. Thus the resolution function given in equation (1) is finite everywhere in momentum–energy space whereas in reality it must cut off at some definite distance from the origin. In the numerical methods of convolution used previously this is unimportant since the integration may be truncated at some convenient point, but in the present analytic method the integration must be taken from $-\infty$ to $+\infty$ over each variable. Thus the use of a cross-section function which becomes infinite at any point will produce a value of the predicted scattered neutron intensity which contains a non-physical contribution from this infinity.

In practice this limitation will become important only at those low values of ω where the cross section varies significantly over the volume swept out by the resolution function along the path in momentum–energy space followed by the experiment. In such cases it may be more convenient to carry out the integration of x, y and z analytically and then integrate over both ω and μ numerically.

I would like to acknowledge several helpful suggestions from Dr J. L. Beeby during the course of this work and discussions with D. H. Saunderson and Dr M. W. Stringfellow.

APPENDIX

The integral

$$I(\mathbf{X}^0)=\int_{-\infty}^{\infty}\exp -\left[\sum_{i=1}^{4}\sum_{j=1}^{4}\{X_iA_{ij}X_j + i\mu(X_i^0+X_i)B_{ij}(X_j^0+X_j)\}\right]\prod_{i=1}^{4}\mathrm{d}X_i \quad (A1)$$

may be readily evaluated by the method of completing the squares in the exponent for each of the variables in turn. The result is

$$I(\mathbf{X}^0)=(E+iF)\exp(G+iH) \quad (A2)$$

where

$$E+iF=\pi^2(\alpha_1\alpha_2\alpha_3\alpha_4)^{-1/2} \quad (A3)$$

$$\alpha_1=C_{11},\quad \mathbf{C}=\mathbf{A}+i\mu\mathbf{B}$$

$$\alpha_2=C_{22}-\frac{C_{12}^2}{C_{11}}$$

$$\alpha_3=C_{33}-\frac{F_1^2}{\alpha_2}-\frac{C_{13}^2}{C_{11}}$$

$$\alpha_4 = C_{44} - \frac{F_2^2}{\alpha_2} - \frac{C_{14}^2}{\alpha_1} - \frac{F_3^2}{\alpha_3}$$

where

$$F_1 = C_{23} - \frac{C_{12}C_{13}}{C_{11}}$$

$$F_2 = C_{24} - \frac{C_{12}C_{14}}{C_{11}}$$

$$F_3 = C_{34} - \frac{F_1F_2}{\alpha_2} - \frac{C_{14}C_{13}}{\alpha_1}.$$

$$G + iH = -i\mu \sum_{i=1}^{4}\sum_{j=1}^{4} X_i^0 B_{ij} X_j^0 + \frac{D_1^2}{\alpha_1} + \frac{D_2^2}{\alpha_2} + \frac{D_3^2}{\alpha_3} + \frac{D_4^2}{\alpha_4}$$

where

$$D_1 = i\mu \sum_{i=1}^{4} B_{1i} X_i^0$$

$$D_2 = \frac{C_{12}D_1}{C_{11}} - i\mu \sum_{i=1}^{4} B_{2i} X_i^0$$

$$D_3 = \frac{C_{13}D_1}{C_{11}} - \frac{F_1D_2}{\alpha_2} - i\mu \sum_{i=1}^{4} B_{3i} X_i^0$$

$$D_4 = \frac{C_{14}D_1}{\alpha_1} - \frac{F_2D_2}{\alpha_2} - \frac{F_3D_3}{\alpha_3} - i\mu \sum_{i=1}^{4} B_{4i} X_i^0.$$

The addition of a term linear in ω allows a parabolic dispersion surface, as found for example in a ferromagnet, to be treated. A constant term in the equation of the dispersion surface allows an energy gap at $\mathbf{Q}=0$. The result of these additions are further terms in equation (A1) which becomes

$$I(\mathbf{X}^0) = \int \exp -\left\{ \sum_{i=1}^{4}\sum_{j=1}^{4} [X_i A_{ij} X_j + i\mu(X_i^0 + X_i) B_{ij} (X_j^0 + X_j)] + i\mu(T(X_4^0 + X_4) + H) \right\} \prod_{i=1}^{4} \mathrm{d}X_i \qquad \text{(A4)}$$

where T and H are constant coefficients.

The result of these integrations is again of the form of equation (A2) and the values of E and F are as before except that

$$D_4 = \frac{C_{14}D_1}{\alpha_1} - \frac{F_2D_2}{\alpha_2} - \frac{F_3D_3}{\alpha_3} - i\mu \sum_{i=1}^{4} B_{4i} X_i^0 - i\mu T$$

and

$$G + iH = -i\mu \sum_{i=1}^{4} X_i^0 B_{ij} X_j^0 + \frac{D_1^2}{\alpha_1} + \frac{D_2^2}{\alpha_2} + \frac{D_3^2}{\alpha_3} + \frac{D_4^2}{\alpha_4} - i\mu(H + T\omega_0).$$

Reference

COOPER, M. J. & NATHANS, R. (1967). *Acta Cryst.* **23**, 357.

Acta Cryst. (1971). A**27**, 410

Neutron Diffraction Effects due to the Lattice Displacement of a Vibrating Quartz Single Crystal

BY R. MICHALEC, L. SEDLÁKOVÁ, B. CHALUPA AND D. GALOCIOVÁ
Nuclear Research Institute of the Czechoslovak Academy of Sciences, Řež, near Prauge

AND V. PETRŽÍLKA
Faculty of Mathematics and Physics of the Charles University, Prague

(*Received* 19 *January* 1970)

The time modulation of neutrons diffracted by a quartz single crystal is investigated. The experimental results agree with the aberration and with the Doppler effect caused during neutron diffraction by vibrations of a single crystal.

Introduction

In diffraction experiments, neutrons with a wavelength of $\lambda = 1$ to 2 Å are conventionally used. These neutrons with velocities of 4×10^5 to 2×10^5 cm.sec^{-1} are also suitable for the investigation of dynamical effects together with the displacement of crystallographic planes and its influence upon the process of neutron diffraction. These dynamical effects are caused by two physical processes. The first is the vector addition of neutron velocity and the velocity of lattice-plane displacement, *i.e.* the aberration effect; the second represents the relative change of neutron wavelength, *i.e.* the Doppler effect. They can be observed in the course of neutron